

Magnetic Field Induced Orientation in Diblock Copolymers with One Crystallizable Block

T. Grigoro[†], S. Pispas,[‡] N. Hadjichristidis,[§] and T. Thurn-Albrecht^{*,†}

Fachbereich Physik, Martin-Luther-Universität Halle-Wittenberg, Hoher Weg 8, 06120 Halle (Saale), Germany; Theoretical and Physical Chemistry Institute, National Hellenic Research Foundation, 48 Vass. Constantinou Ave. 11635 Athens, Greece; and Department of Chemistry, University of Athens, Panepistimiopolis, Zografou, 15771 Athens, Greece

Received January 14, 2005; Revised Manuscript Received April 28, 2005

ABSTRACT: Using wide-angle X-ray scattering, we show that diblock copolymers with one crystallizable block can be oriented by crystallization in a strong magnetic field ($B = 7$ T). The resulting structure consists of a stack of alternating crystalline and amorphous layers of different chemical compositions with the layer normal being oriented perpendicular to the applied field. As a necessary prerequisite the crystallization process has to start with a high nucleation density. Orientation parameters of about $S \approx -0.3$ have been achieved. This approach presents a novel route to produce oriented chemically heterogeneous nanostructured materials.

Introduction

Because of their ability to spontaneously develop patterns on a nanometric scale, block copolymers have attracted much attention as prominent systems for nanotechnological applications based on self-assembly.¹ In this context, the limited control over order and orientation of the microphase domains achievable today poses severe restrictions on possible usages of these systems. While alignment of block copolymer microdomains in shear flow is well established but in many circumstances difficult to use,² it is only recently that the potential of electromagnetic fields for alignment of block copolymers has been fully realized.^{1,3–6} Electric field induced alignment has been shown to be especially useful in thin films which are of interest as templates for artificial nanostructures.^{7,8} For systems in which the two blocks have different dielectric constants, the electric field couples to the anisotropic shape of cylindrical or lamellar block copolymer microdomains and induces orientation of the internal interfaces along the field direction,^{4,9} while on a molecular (segmental) level the material is isotropic. A different handle on orientation is available in materials which exhibit anisotropic susceptibility due to an anisotropic molecular structure. This has recently been used in experiments on block copolymers containing a liquid crystalline component whose orientation is coupled to the orientation of the interfaces between microdomains. Magnetic field induced alignment has been realized on cylindrical systems of this kind.^{10,11} Similar alignment effects have also been demonstrated for semicrystalline polymers during crystallization from the melt in the presence of a strong magnetic field. Orientation in this case is caused by the molecular anisotropy of polymer crystals.^{12–14} In this paper, we demonstrate that these latter effects can also be employed to induce orientation in block copolymer systems, in which a chemically

heterogeneous structure is formed due to crystallization of one block. The resulting structure is lamellar.

Magnetic Field Effects

If a magnetic field is applied to a semicrystalline polymer during crystallization, a magnetic torque will act on the growing crystals due to their anisotropic structure which goes along with an anisotropic diamagnetic susceptibility. If the corresponding orientation-dependent energies are large compared to thermal energy and the mobility of the growing crystals in the viscous surrounding is sufficient, the material tends to orient perpendicular to the direction of the applied field with the principal axis of the susceptibility tensor $\tilde{\chi}$, which corresponds to the lowest susceptibility. This effect does not necessarily lead to macroscopic alignment since the magnetic field does not change the spherulitic growth mode of semicrystalline polymers, which leads inherently to isotropy on a macroscopic level. To get overall alignment, the size of spherulites has to be restricted to the inner hedritic core consisting of a stack of approximately parallel lamellae.¹⁴ This can be achieved by high nucleation density, e.g., by self-seeding.¹⁵

Poly(ethylene oxide) (PEO), the crystallizable block of the block copolymer used, forms a crystal with monoclinic unit cell (see Figure 1; lattice parameters: $a = 0.805$ nm, $b = 1.304$ nm, $c = 1.948$ nm, $\beta = 125.4^\circ$).¹⁶ One of the principal axes of $\tilde{\chi}$ is parallel to \bar{c} , which corresponds to the direction of the chain axis (eigenvalue $\chi_{||}$). The other two axes, χ_1 and χ_2 , are orthogonal to the \bar{c} -direction. Under the simplifying assumption $\chi_1 \approx \chi_2 = \chi_{\perp}$, the magnetic contribution of a crystal to the free energy can be written as

$$G_{\text{mag}}(\vartheta) = \frac{-VB^2\Delta\chi \cos^2 \vartheta}{2\mu_0} \quad (1)$$

where $\Delta\chi = \chi_{||} - \chi_{\perp}$, V is the volume of the object under consideration, χ_0 is the permeability of the vacuum, and ϑ denotes the angle between the magnetic flux density \bar{B} and the \bar{c} axis. For PEO, $\Delta\chi$ is negative, which results in a state of lowest free energy for $\vartheta = \pi/2$; i.e., at equilibrium the chain axis is oriented perpendicular to

[†] Martin-Luther-Universität Halle-Wittenberg.

[‡] National Hellenic Research Foundation.

[§] University of Athens.

* To whom correspondence should be addressed. E-mail: thurn-albrecht@physik.uni-halle.de.

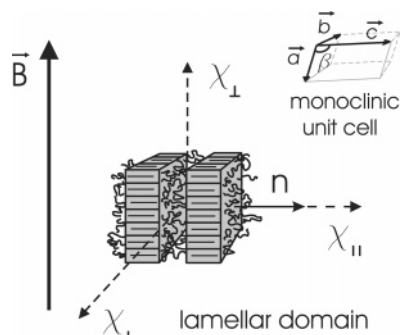


Figure 1. Schematic drawing of oriented crystalline lamellae in a magnetic field. Because of their anisotropic structure, the lamellar crystallites tend to align with the axis of lowest susceptibility perpendicular to the direction of the magnetic field, \vec{B} . For PEO, this axis corresponds to the direction of the polymer chain in the crystal.

the direction of \vec{B} , as schematically shown in Figure 1. An exact value for $\Delta\chi$ of PEO is not known, but from tabulated data¹⁷ it can be estimated that $\Delta\chi < -4.85 \times 10^{-6}$.

Generally, the effect of the external field on an individual molecule is weak. $\Delta G = G(0) - G(\pi/2)$ becomes comparable with thermal energy ($k_B T \approx 4.46 \times 10^{-21}$ J for $T = 50$ °C) for a crystal with a volume corresponding to a sphere with a diameter of at least 50 nm. The field will therefore have no significant effect on nucleation but will act later during growth once the crystal has reached a sufficient size.

Experimental Section

Poly(ethylene oxide-*b*-butadiene) was synthesized by anionic polymerization methods, using THF as the solvent and phosphazine base as the ethylene oxide polymerization promoter, leading to a 1,2-microstructure of the PB block.¹⁸ The block copolymer had weight-average molecular weight $M_w = 17\,800$ g/mol (as determined by combination of size exclusion chromatography and H NMR measurements) and a polydispersity index $M_w/M_n = 1.04$. The composition, determined by NMR, was 93 wt % PEO. For comparison, some experiments were performed with pure homopolymer poly(ethylene oxide) (PEO) having a weight-average molar mass $M_{wt} = 30\,800$ g/mol. A Perkin-Elmer DSC 7 was used for calorimetric experiments to determine the apparent melting temperature range and to estimate the time necessary for complete crystallization at different temperatures T_c . To determine the morphology of the diblock copolymer, small-angle X-ray scattering (SAXS) measurements were performed with a Kratky camera using slit collimation. The setup was equipped with a temperature-controlled sample holder. Data were desmeared applying the algorithm developed by Strobl.¹⁹ The nucleation density as obtained after different thermal treatments prior to crystallization was qualitatively observed by polarized light microscopy with an Axioplan 2 microscope (Zeiss) equipped with a hotstage (Linkam TMS 600). To characterize the state of orientation of the samples, 2D-WAXS experiments were performed using a setup with a rotating anode and an image plate detector (Schneider, Offenburg, Germany). Measurements were performed in transmission geometry at normal incidence. Samples for scattering experiments were prepared as disks with a thickness of about 0.5 mm. To enable well-defined temperature programs during crystallization, a custom-designed heatable sample cell was used in a 7 T Bruker NMR magnet.¹⁴

Results and Discussion

Microphase Structure. Figure 2 shows two sets of small-angle X-ray scattering (SAXS) data obtained from an isotropic diblock copolymer sample in the crystalline

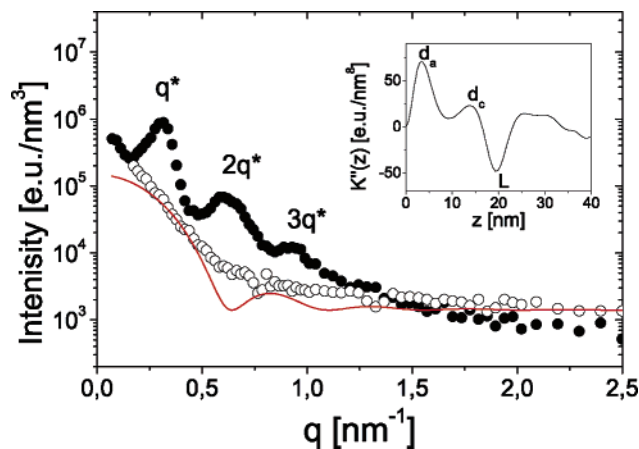


Figure 2. Small-angle X-ray scattering patterns of poly(ethylene oxide-*b*-butadiene) sample in the amorphous ($T = 65$ °C, open symbols) and the crystalline state ($T = 50$ °C, filled symbols). At high temperature the sample forms disordered micelles.²⁰ The solid line shows for comparison the form factor of a sphere with a radius of 7 nm. For the crystalline state three peaks at q^* , $2q^*$, and $3q^*$ indicate a lamellar structure. The interface distribution function $K''(z)$ of the lamellar structure is shown in the inset. The three peaks correspond as indicated to the thicknesses of the amorphous (d_a) and crystalline layers (d_c) and to the long period (L).

($T = 50$ °C) and the amorphous state ($T = 65$ °C). The SAXS data, plotted as intensity vs scattering vector $q = (4\pi/\lambda) \sin \theta$, where 2θ is the scattering angle, indicate a disordered micellar structure²⁰ in the molten state and a stacked lamellar morphology after crystallization. Since in the system under study contrast comes mainly from the large difference in electron density between crystalline PEO and amorphous PB, we conclude that the original microstructure is overwritten by crystallization, leading to a lamellar structure consisting essentially of crystalline PEO and amorphous PB layers with the latter containing a certain amount of amorphous PEO ($\rho_{\text{PEO,c}}^e = 410 \text{ nm}^{-3}$, $\rho_{\text{PEO,a}}^e = 369 \text{ nm}^{-3}$, $\rho_{\text{PB,a}}^e = 298 \text{ nm}^{-3}$). The radius of the micelles, $R \approx 7$ nm, was determined by comparison with the form factor of a sphere. Deviations at small q can be explained by the presence of an interference peak which could not be well resolved with the apparatus used. To determine the inner structure of the lamellar stacks in the crystallized sample, the interface distribution function, $K''(z) = \langle \rho'(0)\rho'(z) \rangle$, was calculated.²¹ $K''(z)$ is proportional to the probability distribution of the distances between amorphous–crystalline interfaces. It allows a determination of the average thickness of the amorphous and crystalline layers and of the long period (see Figure 2, inset: $d_a = 3.6$ nm, $d_c = L - d_a = 15.7$ nm, and $L = 19.3$ nm). The linear crystallinity amounts to $d_c/L = 0.81$, i.e., somewhat smaller than the PEO volume fraction of the block copolymer of 91% (assuming for PEO:¹⁶ $\rho^{\text{CR}} = 1.23 \text{ g/cm}^3$). This indicates that the amorphous layers contain indeed a certain amount of PEO as expected.

Magnetic Field Induced Alignment. A typical crystallization program leading to oriented samples consisted of the following steps: The sample was heated with a rate of 10 K/min to a temperature T_{max} above the apparent melting temperature, annealed there for 6 min, and then quickly cooled to room temperature with a rate of ~ 25 K/min. Similar results were obtained for isothermal crystallization at elevated temperatures. In all cases the temperature T_{max} had to be chosen only

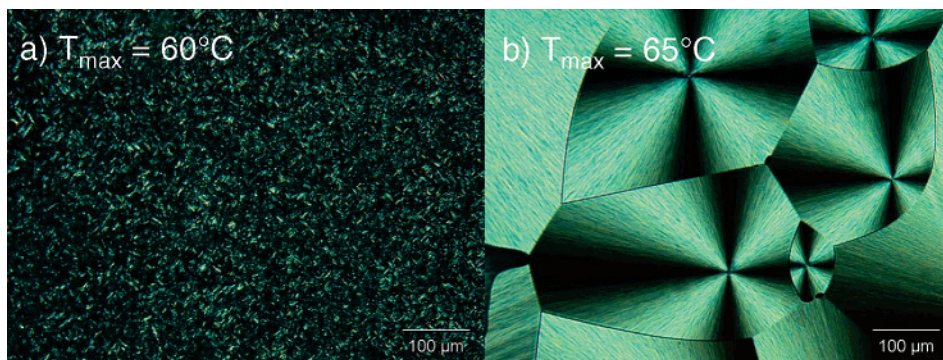


Figure 3. Optical micrographs of poly(ethylene oxide-*b*-butadiene) samples crystallized within a few minutes (at $T_c = 40$ °C) after annealing at different T_{\max} temperatures. The density of nuclei initiating crystallization depends strongly on the thermal history. Heating the samples just above the melting temperature results in a high number of nuclei via self-seeding (a). Only samples with high nucleation density are oriented if a magnetic field is present during crystallization. A T_{\max} only 5 °C higher leads to a strong decrease of the nucleation density, resulting in large spherulitic structures (b).

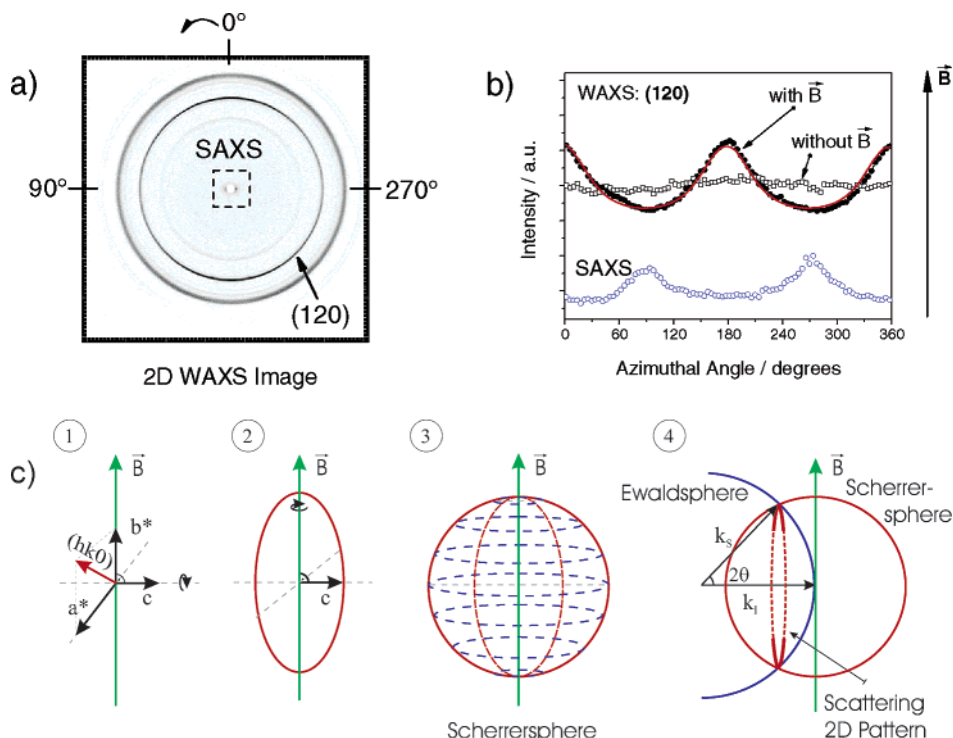


Figure 4. (a) Anisotropic 2D WAXS scattering pattern from a sample crystallized in a magnetic field. (b) Azimuthal WAXS scans of the (120) reflection of poly(ethylene oxide-*b*-butadiene) samples rapidly crystallized with and without magnetic field ($T_{\max} = 60$ °C). The solid line is obtained from a model calculation assuming a Gaussian orientation distribution with an orientation parameter $S = -0.33^{14}$ (for perfect orientation $\vec{c} \perp \vec{B}$: $S = -0.5$). An azimuthal scan of the SAXS intensity is also shown (integrated over the q range from 0.81 to 1.1 nm $^{-1}$). (c) Construction of the scattering pattern as observed in a 2D WAXS measurement. For uniaxial orientation ($\vec{c} \perp \vec{B}$ and no preferred orientation of \vec{a} and \vec{b}) an $(hk0)$ reflection shows a typical azimuthal distribution with maximum intensity in the direction of \vec{B} (further explanation given in the text).

slightly higher than the apparent melting temperature such that large nucleation rates were achieved by self-seeding. Subsequently, the samples were investigated with wide-angle X-ray scattering (WAXS) at ambient temperature. Since the range of temperatures ΔT_{\max} for which strong self-seeding occurs is small ($\Delta T_{\max} \approx 1$ K), it is essential to determine the appropriate temperature by optical microscopy. Exemplary results are shown in Figure 3.

A 2D WAXS pattern obtained from an oriented sample of PEO-*b*-PB is shown in Figure 4a, crystallized in a magnetic field $B = 7$ T. The observed pattern is anisotropic, indicating an oriented structure. Close inspection shows that also the tail of the SAXS intensity, visible close to the beam stop, is anisotropic. An azimuthal scan of the integrated intensity of the (120)

reflection is shown in Figure 4b together with the analogous data, obtained from a sample crystallized without magnetic field. The azimuthal distribution of the SAXS intensity is also shown indicating an orientation of the lamellar normal perpendicular to \vec{B} . The WAXS pattern can be understood as follows (since only the strongest reflection of PEO, (120), is used for the analysis, only this reflection is discussed here; cf. ref 14 otherwise): For the monoclinic unit cell of PEO, the reciprocal lattice is also monoclinic with \vec{b}^* being parallel to \vec{b} . Reciprocal vectors \vec{a}^* and \vec{b}^* define a plane perpendicular to \vec{c} (Figure 4c, part 1). If the unit cell is oriented with the \vec{c} -axis (the chain axis) perpendicular to the magnetic field, \vec{B} , without \vec{a}^* and \vec{b}^* showing a preferred orientation, the (120) reflection, as a result from the two averaging procedures illustrated in Figure

4c, parts 2 and 3, is distributed nonhomogeneously over a sphere with high intensity at the poles and lower intensity at the equator. The scattering pattern observed on the detector in an experiment with transmission geometry follows from the Laue condition $[\vec{q}_{hkl}] = \vec{k}_S - \vec{k}_I$, where \vec{k}_I and \vec{k}_S are the wave vectors of the incident and the scattered X-ray beam (Figure 4c, part 4). The intensity distribution on the intersection of the Ewald sphere with radius $|\vec{k}_I|$ and the sphere corresponding to the $(hk0)$ reflection gives the intensity observed on the 2D detector. An azimuthal scan over the ring, corresponding to a $(hk0)$ reflection, therefore shows two peaks in the direction of \vec{B} with a finite width and a finite offset even for perfect orientation, exactly as observed in our data.

As mentioned, the conditions necessary for alignment to occur in the block copolymer system are similar to what was observed for homopolymers, indicating that the same alignment mechanism is responsible for the phenomena observed. In the block copolymer case orientation of the crystallites naturally also leads to alignment of the microphase structure resulting from crystallization. As experiments with other block copolymers of the same kind but with different volume fractions have shown, it is important that the original microphase-separated structure consists of micelles which do not form a connected structure. Cylindrical or lamellar polybutadiene microdomains would reduce the mobility of the growing crystals to an extent which makes it difficult to produce well-aligned lamellar structures after crystallization. On the other hand, the approach could be well extended to samples crystallizing from the disordered state.

Conclusions

We demonstrated a novel approach to realize alignment of block copolymer microstructures using an external magnetic field. Explicitly, we have shown that by crystallizing a diblock copolymer in a magnetic field an oriented, chemically nanostructured material can be produced. A critical point is the restriction of spherulitic growth by high nucleation density, which here has been achieved by self-seeding. An alternative option would be the addition of nucleating agents.²² While the resulting orientation is similar as in the case of an amorphous-amorphous diblock copolymer oriented in an electric field, the principle used for alignment is based on a different mechanism leading to orientation during crystal growth. The effects shown here are of potential interest for functional, partially crystalline polymers.

Acknowledgment. We thank G. Strobl for his general support of the project. We are grateful to R. Thomann for giving us the opportunity to perform the optical microscope measurements and K. Saalwächter for the access to the NMR magnet in the Institute for Macromolecular Chemistry, Albert-Ludwigs-Universität Freiburg. Technical help from B. Heck, F. Ebert, and S. Hugger is gratefully acknowledged. For the analysis of 2D scattering data, we used FIT2D software written by A. P. Hammersley, ESRF. This work is supported by the EC under Contract HPRN-1999-00151.

References and Notes

- (1) Park, C.; Jongseung Yoon, J.; Thomas, E. L. *Polymer* **2003**, *44*, 6725.
- (2) Hamley I. W. *The Physics of Block Copolymers*; Oxford University Press: New York, 1998.
- (3) Amundson, K.; Helfand, E.; Davis, D.; Quan, X.; Patel, S. *Macromolecules* **1991**, *24*, 6546.
- (4) Amundson, K.; Helfand, E.; Quan, X.; Smith, S. D. *Macromolecules* **1993**, *26*, 2698.
- (5) Thurn-Albrecht, T.; DeRouchey, J.; Russell, T. P.; Kolb, R. *Macromolecules* **2002**, *35*, 8106.
- (6) Böker, A.; Elbs, H.; Hänsel, H.; Knoll, A.; Ludwigs, S.; Zettl, H.; Urban, V.; Abetz, V.; Müller, A. H. E.; Krausch, G. *Phys. Rev. Lett.* **2002**, *89*, 135502.
- (7) Thurn-Albrecht, T.; Schotter, J.; Kästle, G.; Emley, N.; Shibauchi, T.; Krusin-Elbaum, L.; Guarini, K.; Black, C.; Tuominen, M.; Russell, T. *Science* **2000**, *290*, 2126.
- (8) Morkved, T.; Lu, M.; Urbas, A.; Ehrlich, E.; Jaeger, H.; Mansky, P.; Russell, T. *Science* **1996**, *273*, 931.
- (9) DeRouchey, J.; Thurn-Albrecht, T.; Russell, T.; Kolb, R. *Macromolecules* **2004**, *37*, 2538.
- (10) Osuji, C.; Ferreira, P. J.; Mao, G.; Ober, C. K.; Vander Sande, J. B.; Thomas, E. L. *Macromolecules* **2004**, *37*, 9903.
- (11) Hamley, I. W.; Castelletto, V.; Lu, B.; Imrie, C. T.; Itoh, T.; Al-Hussein, M. *Macromolecules* **2004**, *37*, 4798.
- (12) Ezure, H.; Kimura, T.; Ogawa, S.; Ito, E. *Macromolecules* **1997**, *30*, 3600.
- (13) Kimura, T. *Polym. J.* **2003**, *35*, 823.
- (14) Ebert, F.; Thurn-Albrecht, T. *Macromolecules* **2003**, *36*, 8685.
- (15) Wunderlich, B. *Macromolecular Physics*; Academic Press: New York, 1976; Vol. 2.
- (16) Miller R. L. In *Polymer Handbook*, 4th ed.; Brandrup, J., Immergut E. H., Grulke E. A., Abe A., Bloch D. R., Eds.; Wiley-Interscience: New York, 1999; Vol. 1.
- (17) Van Krevelen, D. W. *Properties of Polymers*; Elsevier Science B.V.: Amsterdam, 1990.
- (18) Pispas, S.; Hadjichristidis, N. *Langmuir* **2003**, *19*, 48.
- (19) Strobl, G. *Acta Crystallogr.* **1970**, *26*, 367.
- (20) Schwab, M.; Stühn, B. *Phys. Rev. Lett.* **1996**, *76*, 924.
- (21) Ruland, W. *Colloid Polym. Sci.* **1977**, *255*, 417.
- (22) Kawai, T.; Iijima, R.; Yamamoto, Y.; Kimura, T. *Polymer* **2002**, *43*, 7301.

MA050081P